Ecological Complexity 40 (2019) 100776

Contents lists available at ScienceDirect

Ecological Complexity

journal homepage: www.elsevier.com/locate/ecocom

Fish disease dynamics in changing rivers: Salmonid *Ceratomyxosis* in the Klamath River

Vanessa Schakau[*,a], Frank M. Hilker[a], Mark A. Lewis[b,c]

[a] Institute of Environmental Systems Research, School of Mathematics and Computer Science, Osnabrück University, Osnabrück 49069, Germany
[b] Department of Mathematical and Statistical Sciences, University of Alberta, Edmonton, Alberta T6G 2E9, Canada
[c] Department of Biological Sciences, University of Alberta,Edmonton, Alberta T6G 2E9, Canada

ARTICLE INFO

Keywords:
Climate change
Epidemiological model
Myxozoans
Ceratomyxa shasta
Dam removal

ABSTRACT

The myxozoan parasite *Ceratomyxa shasta* has been identified as the main contributor of mortality in salmon in the Klamath River, California. The life cycle of the parasite is complex, involving a polychaete and a salmonid host. Infection dynamics are greatly influenced by environmental factors, such as temperature and water velocity. If we are to control the disease it is important to predict the impact of environmental scenarios on spore concentration and infection prevalence. Here, we introduce a model based on partial differential equations to study the spore concentration in the river and the infection prevalence of returning salmon. The analysis of the model shows that for current climate conditions, additional dam release can reduce the actinospore concentration up to 48% and the prevalence up to 40% thus providing a potential disease management option. However, the infection risk is likely to increase for future climate conditions by 10–54% and this will lead to an infection level comparable to that of a recent high-disease year. Our simulations show that dam removal cannot be assumed to mitigate the effect of climate change or to have influence on infection prevalence. We show that our detailed model system can be reduced to a simpler exponential dose-response function, which predicts infection levels based on transmission rates, travel time and mean spore concentration, quantities that can be measured *in-situ* or given empirically. The dose-response function may therefore be a useful tool in disease management.

1. Introduction

Myxozoans are a group of aquatic parasites that are known to cause several fish diseases that can have severe economic impact on fisheries and aquaculture (Hallett and Bartholomew, 2011; Okamura et al., 2015). Whirling disease, proliferative kidney disease and enteronecrosis, for example, are three economically important fish diseases caused by a myxozoan parasite (Jones et al., 2015). Several emerging diseases caused by myxozoans have been linked with climate change (Okamura et al., 2015). The life cycle of myxozoans is complex and involves both invertebrate (mainly annelids) and vertebrate hosts (mainly fish).

The myxozoan freshwater parasite *Ceratonova shasta* (syn. *Ceratomyxa shasta*) has been identified as the main contributor of mortality in Chinook (*Oncorhynchus tshawytscha*) and Coho (*O. kisutch*) salmon in the Klamath River, California. In the past decade, the salmon population in Klamath River has continuously declined, in part due to *Ceratomyxosis* (enteronecrosis) that is caused by *C. shasta* (Fujiwara et al., 2011; Stocking et al., 2006; True et al., 2011). The parasite can be found throughout the Pacific Northwest, but its negative impact on native salmon populations is greatest in the Klamath River. Up to 62% of outmigrating juvenile Chinook salmon are infected with *C. shasta* (Jones et al., 2015) and, combined with high disease-induced mortality, the disease leads to reduced numbers of both outmigrating juvenile salmon and returning adults (Fujiwara et al., 2011; Hallett et al., 2012; Stocking et al., 2006). However, quantifying the impact on wild fish populations is difficult due to the lack of long-term data (Okamura et al., 2015).

C. shasta has a complex life cycle, meaning that it switches between two hosts and two spore stages (Fig. 1): the invertebrate polychaete *Manayunkia speciosa* releases actinospores into the water, where they infect the salmon host. After successful infection, the parasite develops into the myxospore stage, which is released when the infected salmon dies a natural or disease induced death. The myxospores re-infect the freshwater polychaete living in the sediment layer of the river.

Due to the high impact of *C. shasta* in the Klamath River, managing

* Corresponding Author. Present address: Institute for Chemistry and Biology of the Marine Environment, University of Oldenburg, 26129 Oldenburg, Germany.
E-mail address: vanessa.schakau@uol.de (V. Schakau).

https://doi.org/10.1016/j.ecocom.2019.100776
Received 4 April 2019; Received in revised form 30 July 2019; Accepted 31 July 2019
Available online 27 August 2019
1476-945X/

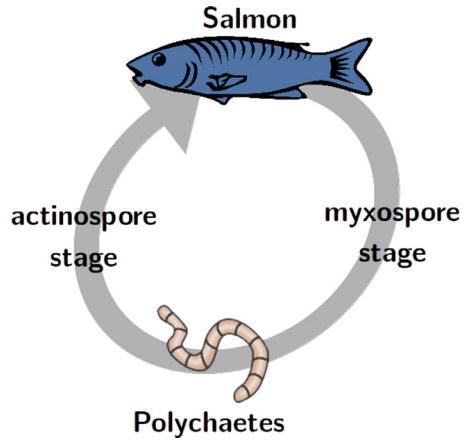

Fig. 1. The complex life cycle of myxozoan freshwater parasite *Ceratomyxa shasta* involves two hosts and two spore stages: the invertebrate polychaete *Manayunkia speciosa* releases actinospores into the water, where they infect the salmon host. After successful infection, the parasite develops into the myxospore stage, which is released when the infected salmon dies. The myxospores re-infect the freshwater polychaete host living in the sediment layer of the river.

the disease has a high priority. Recent studies investigate the efficacy of removing adult carcasses to reduce the myxospore input into the system (Foott et al., 2016) and flow manipulation in order to reduce the polychaeta density (Alexander et al., 2014) or to reduce the spore concentration (Bartholomew et al., 2016). The infection dynamics are greatly influenced by environmental factors such as temperature and water velocity. Future climate scenarios in the Klamath River predict significant differences in both temperature and precipitation patterns compared to current conditions (Perry et al., 2011; Ray et al., 2015) and are likely to affect spore concentration and disease risk. Besides climate change, the proposed removal of dams in the Klamath River Basin is assumed to affect fish health adversely due to aggravation of infection risk (Hurst et al., 2012). Therefore, determining the effect of changing environmental conditions on the disease dynamics is crucial to aid disease control and mitigation. Furthermore, knowing about the effect of environmental parameters on infection prevalence can be used for targeted intervention.

Mathematical models can help to identify the important processes and critical points in the disease cycle and can help to evaluate the efficiency of disease management options before implementation. However, the testing and implementation of predictive models for aquatic diseases is challenging due to a lack of data and the complexity of host-parasite interactions (Ray et al., 2015).

A predictive model ensemble for *Ceratomyxosis* in the Klamath River was used to analyse disease dynamics under future climate change scenarios (Ray et al., 2015). The modelling approach combined statistical and epidemiological models with meta-analysis data to predict the concentration of the two spore stages and the infection in juvenile salmon and the polychaete host. An ordinary differential equation (ODE) model for *Ceratomyxosis* in the Klamath River was used to study the influence of temperature and discharge on the parasite-induced mortality in juvenile salmon (Fujiwara, 2014). However, neither model considers the spatial aspects of fish migration or spore concentration which should play a role in determining disease dynamics. The focus of the Fujiwara (2014) study is on predicting the mortality in juvenile salmon. Moreover, previous models largely ignore the role of adult salmon in the infection dynamics. As infected adult carcasses produce myxospores that re-infect the polychaete host, they represent an important link in the pathogen's life cycle. The potential significance of adult salmon in the infection cycle has also been mentioned by Ray (2013) and Fujiwara (2014). More recently, the role of infected adult salmon in the infection cycle and the possibility of removing adult carcasses to reduce the myxospore input into the river, so as to diminishing the disease induced mortality of juvenile salmon in the following spring, has been investigated by Foott et al. (2016). However, they concluded that there are little effects on myxospore concentration by removing carcasses.

In order to gain a better understanding of the myxozoan disease dynamics, including the effects of spatial migration, adult salmon, climate scenarios and dam options, we consider a complex system including dynamic processes such as hydrodynamics, environmental conditions and host-parasite interactions, where each mechanism could be studied by a model on its own. In an attempt to balance realism and analytical tractability, we simplify this complex system to one of three partial differential equations (PDEs) which retain, nevertheless, the dynamically important mechanisms. Our approach is based on a spatial one-dimensional epidemiological model with advection to study the actinospore concentration in the river and the infection prevalence of returning salmon. While our PDE model is instrumental in gaining insight into the interacting processes, disease management is more interested in straight-forward predictions of disease risk based on data available or easy-to-parametrize models. To this end, we demonstrate how our PDE model can be transformed into a dose-response model.

Dose-response models are widely used in quantitative microbiological risk assessment. They are used to evaluate the risk of infection of susceptible hosts after a single-dose pathogen exposure. For example, they have been applied to infectious gastroenteritis caused by several pathogens (Teunis et al., 1999), *Mycobacterium tuberculosis* (Huang and Haas, 2009), SARS Coronavirus (Watanabe et al., 2010) and Influenza A Virus (Watanabe et al., 2011). The classical models used to calculate the prevalence of infection are the exponential and the beta-Poisson dose-response model (Haas et al., 1999). The development of a dose-response model for *Ceratomyxosis* will be of assistance in order to approximate the infection risk of the years returning salmon population and to aid disease management.

In this paper we carefully connect the model to underlying biological and physical assumptions and then analyse the model under different water flow settings and temperatures to explore the effect of environmental change on the disease dynamics. To validate our model, we compare our predictions to field measurements. We analyse the applicability of flow manipulation as a disease management option and we then present future projections under both climate change and dam removal scenarios. Finally, we demonstrate how our model system can be reduced to a single equation, namely the dose-response model, which is applicable as a disease management tool.

2. Model description

The aim of the model is to predict the prevalence of infection in the adult salmon host. To this end we develop a coupled spatial eco-epidemiological modeling system that mainly consists of two parts, namely the actinospore distribution model and the salmon infection model. In this section we first describe the model study area and the assumptions that are made for the spatial model (Section 2.1). Second, we describe the composite parameters, mainly influenced by water temperature and discharge (Section 2.2), that are used as input parameters for the hereinafter introduced state variables describing the actinospore distribution (Section 2.3) and the infection dynamics (Section 2.4). A conceptual diagram of the model is shown in Fig. 2.

2.1. Model study area

The study area covers the part of the Klamath River affected by *C. shasta* ranging from the Iron Gate Dam (IGD) downstream to the confluence with the Scott River (SR). The area is modelled in one spatial dimension and it is divided into three zones following the descriptions of Stocking and Bartholomew (2007), Bartholomew et al. (2007) and Ray et al. (2015) (Fig. 3):

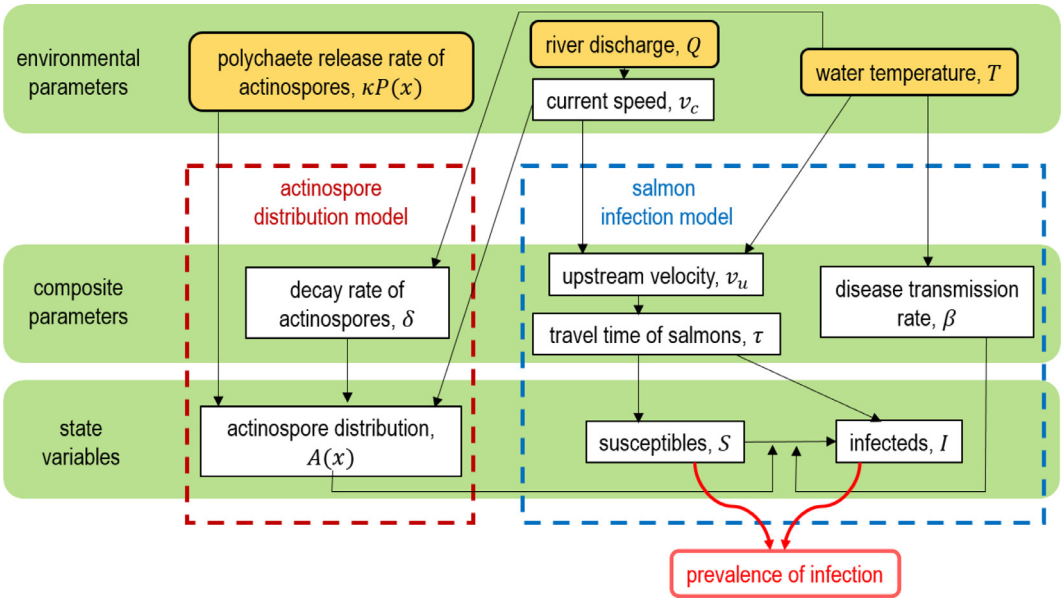

Fig. 2. Conceptual diagram of the model. The number of infected polychaetes $P(x)$, river discharge Q and water temperature T present the environmental input parameters of the model (yellow boxes). All other (biophysical) parameters are derived from these. The actinospore model (red rectangle) predicts the actinospore distribution in the model area. This distribution is used as input for the salmon infection model (blue rectangle) to predict the prevalence of infection in returning salmon. (For interpretation of the references to color in this figure legend, the reader is referred to the web version of this article.)

I Spawning region: High densities of adult salmon are observed in this region of habitat immediately below IGD (River kilometer 306 to 290);
II Polychaete habitat: High densities of infected polychaetes, which release actinospores, are found in this region of the confluence with Shasta River (River kilometer 290 to 278);
III Infection zone: High actinospore densities are measured in the region downstream from the polychaete habitat down to the confluence with Scott River (River kilometer 278 to 229).

We assume that the zones are defined clearly, even though the transitions between the zones may be gradual. For simplification of our mathematical description we transform the spatial extent of the modelled area to $0 \le x \le L$, where the position of the IGD is at $x = 0$ and the downstream boundary at the confluence with Scott River is at $x = L$. We define the reach of the spore release area (zone II) to be located in the region $H_0 \le x \le H_L$, where $0 < H_0 < H_L < L$.

The river discharge Q (given in $\mathrm{m^3\,s^{-1}}$) governs the river velocity v_c (in $\mathrm{m\,s^{-1}}$). We approximate the connection between these two parameters according to a power law relationship described by Govers (1992):

$$v_c = aQ^b\,. \tag{1}$$

Due to its natural structure, the geometry of the Klamath River varies within the river course. To reduce the complexity of the model, we approximate the river by a spatially homogeneous line. Consequently, we average the parameters given by Perry et al. (2011) for the study area to give typical values of $a = 0.2067\,\mathrm{s^{b-1}\,m^{1-3b}}$ with a 95% confidence interval of $[0.1755\,\mathrm{s^{b-1}m^{1-3b}};\ 0.2553\,\mathrm{s^{b-1}m^{1-3b}}]$ and $b = 0.37$ with [0.36; 0.39]. To match the units, the dimension of the parameter a depends on the value of the dimensionless parameter b.

2.2. Influence of environmental parameters

The water temperature is a critical factor that affects fish physiology as well as each phase of the parasites' life cycle. As a consequence, water temperature is one of the main drivers of disease dynamics. A positive relationship between temperature and mortality from *C. shasta* was first described by Udey et al. (1975). Increased temperatures lead to increased transmission rates (Ray, 2013) but also to shorter life times of actinospores (Bjork, 2010; Foott et al., 2007). Since varying temperature affects the disease dynamics both directly and indirectly (e.g. host distribution and density, duration/timing of host-parasite interactions), the net effect of changing environmental conditions is difficult to predict.

The river discharge, and thus the water velocity, have direct and indirect effects on disease dynamics. It affects both, the actinospore distribution and the travel time of salmon and therefore the exposure duration. Moreover, the water velocity is thought to influence the transmission rate (Bjork and Bartholomew, 2009; Ray, 2013) and the polychaete distribution (Bartholomew et al., 2007) additionally.

Little is known about the influence of environmental parameters on other factors such as the polychaete population, actinospore release or the disease progression. For this reason, we restrict ourselves to the incorporation of water temperature and/or velocity on (i) the decay rate of actinospores, (ii) the travel time of migrating salmon and (iii) the transmission rate in our model. The influence of the environmental parameters on the different model mechanisms is summarised in Fig. 2.

2.2.1. Decay rate of actinospores

The life time of actinospores in water is strongly correlated to the temperature (e.g. Bjork, 2010; Foott et al., 2007; Ray et al., 2015). At 4 °C, actinospores persist for about 7 days and at 20 °C for about 4 days. Here, for simplicity, we assume a linear relationship of life time of actinospores with temperature T. The relative decay rate δ corresponds to the inverse of the average life time and can be written as

$$\delta(T) = \frac{\lambda}{\mu - \nu T} \quad \forall \quad T \le 40\,^{\circ}\mathrm{C} \tag{2}$$

where the constants $\lambda = 16\,^{\circ}\mathrm{C\,d^{-1}}$, $\mu = 124\,^{\circ}\mathrm{C}$ and $\nu = 3$ have been chosen to fit the two data points mentioned above and to give integer numbers for the ease of visual appearance.

2.2.2. Upstream migration speed and travel time of salmon

The water temperature and the water flow have a significant effect on the energy reserves, and therefore on the migration velocity, during upstream migration of adult salmon (e.g. Salinger and Anderson, 2006; Standen et al., 2004). For Chinook salmon, the maximum swim speed of

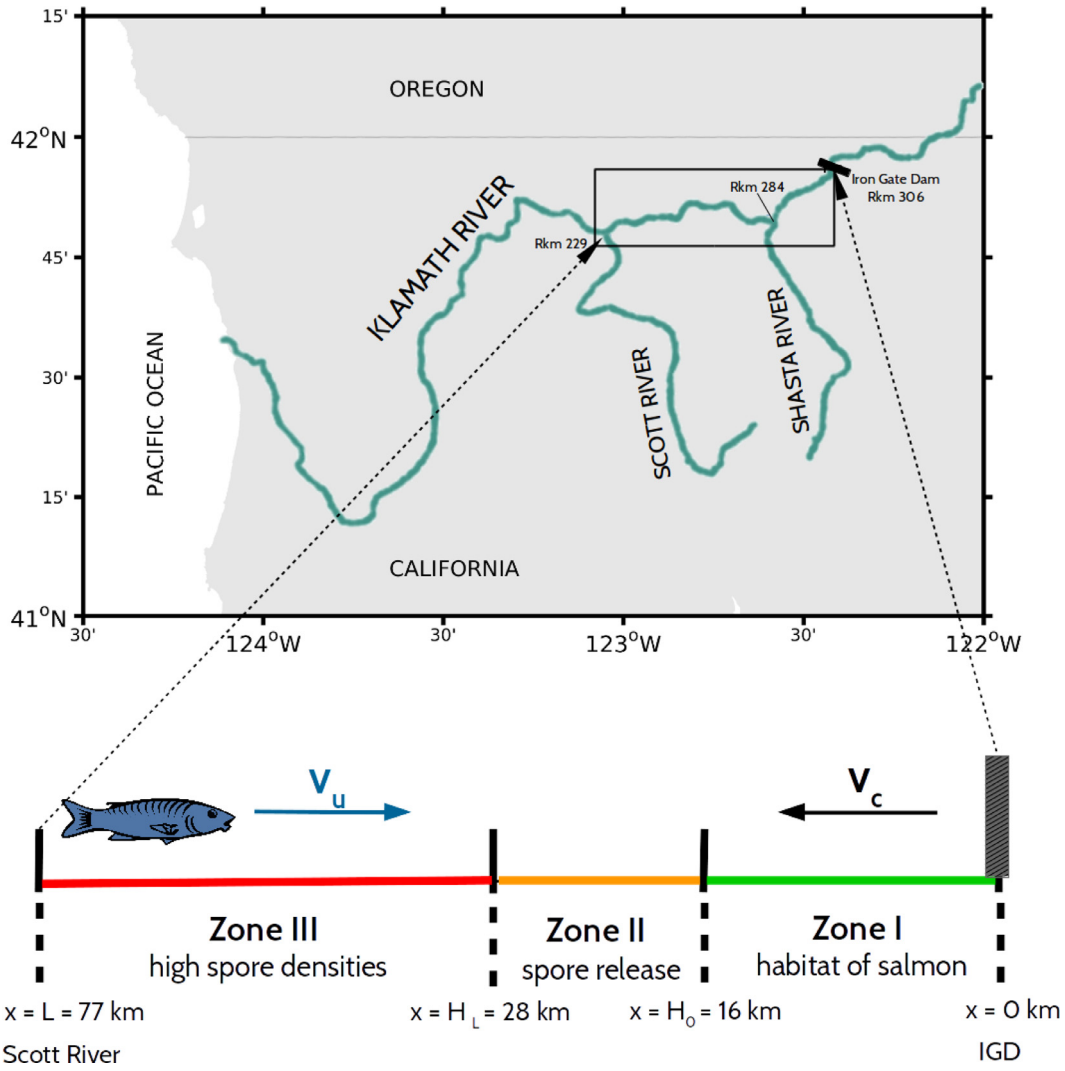

Fig. 3. Location of the model area in the Klamath River, California, (top) and spatial zoning of the model (bottom). The rectangle indicates the model reach. The upstream boundary is given by the Iron Gate Dam (IGD), the confluence of the Klamath River with the Scott River representing the downstream boundary of the model. The model area is divided into three zones: (I) The spawning area of salmon right below IGD; (II) The polychaete habitat where actinospores are released into the water column in the area around the confluence with Shasta River; (III) The infection zone where high densities of actinospores are found down to the confluence with Scott River. The upstream migration speed of salmon v_u is determined by the encountered current speed v_c.

about one body length per second occurs at $T_{opt} = 16.3$ °C and decreases above and below this temperature. Since salmon are efficient at compensating increased water velocities, the water flow has a weaker effect on the migration speed than the temperature has (Salinger and Anderson, 2006). Following Salinger and Anderson (2006), we approximate the migration of adult salmon by a mean upstream velocity v_u in km d^{-1} that depends on the water temperature T and the encountered current speed v_c in km d^{-1} which could be expressed in terms of discharge according to Eq. (1):

$$v_u(T, v_c) = v_u^0 + \eta T - \theta v_c \tag{3}$$

with

$$\begin{cases} v_u^0 = 27.3\,\text{km d}^{-1},\ \eta = 2.0\,\text{km d}^{-1}\text{°C}^{-1},\ \theta = 0.25 & \text{if} \quad T \le T_{opt}\,, \\ v_u^0 = 100.7\,\text{km d}^{-1},\ \eta = -2.5\,\text{km d}^{-1}\text{°C}^{-1},\ \theta = 0.25 & \text{if} \quad T > T_{opt}\,. \end{cases}$$

The migration velocity increases with temperature up to the optimum T_{opt} and then decreases with higher temperatures. We define the travel time τ of salmon in the river section to be proportional to the inverse of the upstream migration velocity v_u. The shortest travel time occurs at T_{opt} and increases with increasing stream discharge Q (Fig. 4).

It should be noted that the studies by Salinger and Anderson (2006) have been performed in the Columbia River. However, their results are similar to observations that have been made in other studies for different salmon and trout species, including both field experiments in

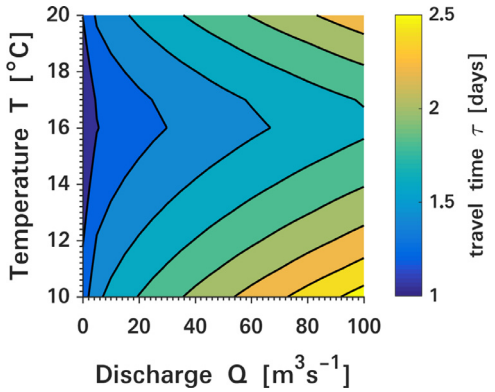

Fig. 4. Travel time τ of salmon through the river section as a function of the river discharge Q and the water temperature T can be derived from the upstream migration velocity v_u (see Eqs. (1) and (3)).

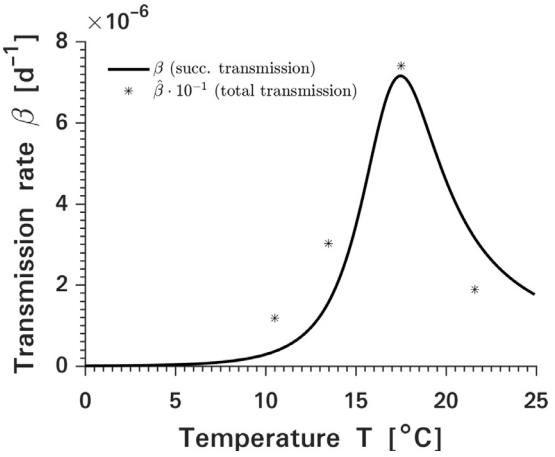

Fig. 5. Successful transmission β as a function of the water temperature T. The function is fitted to measurements describing the total transmission rate $\hat{\beta}$ given by Ray and Bartholomew (2013) (*).

other river systems and laboratory studies (Salinger and Anderson, 2006). Since there is no empirical formulation available describing the functional relationship of temperature, water velocity and adult salmon migration speed in the Klamath River, we here assume the same approach presented by Salinger and Anderson (2006).

2.2.3. Transmission rate

The transmission of microparasites in the aquatic environment is influenced by abiotic factors, such as temperature and water velocity. For *C. shasta*, Ray and Bartholomew (2013) showed that the total transmission rate, here denoted as $\hat{\beta}$, increases with water temperature up to $T = 18$°C and decreases above this value. It should be noted that we assume that not all transmitted actinospores successfully initiate an infection and we therefore distinguish between the total transmission rate $\hat{\beta}$ and the successful transmission rate β, which we assume to be approximately one tenth of the total transmission rate (Fujiwara, 2014). To estimate the successful transmission rate β as a function of the water temperature T, we assume the following functional relationship (Eq. (4)) and fit it to the data points given by Ray and Bartholomew (2013) using the least squared-error method (Fig. 5).

$$\beta(T) = \frac{\varphi(T+\sigma)}{T_0 + \psi \exp(-\omega \cdot T)} \tag{4}$$

The constants and the corresponding standard deviations of the fitted parameter can be found in Table 1.

Besides the water temperature, the water velocity v_c was found to affect the transmission rate (Bjork and Bartholomew, 2009). However, due to the relatively small effect of water velocity on the transmission rate compared to the temperature we focused only on incorporating the effect of temperature.

Table 1
Estimated parameters and their standard deviations for the successful transmission rate β (Eq. (4)). To fit the data points given by Ray and Bartholomew (2013) the least squared-error method was used.

Parameter	Value	Standard deviation
φ	$1.4 \times 10^{-9}\,\mathrm{d}^{-1}$	$0.2 \times 10^{-9}\,\mathrm{d}^{-1}$
σ	8.3×10^{3} °C	1.2×10^{3} °C
$T_0 - T$	− 18 °C	0.3 °C
ψ	2.7×10^{3} °C	0.2×10^{3} °C
ω	0.4 °C^{-1}	0.006 °C^{-1}

2.3. Actinospore distribution model

Little is known about polychaete's life cycle and the influence of environmental parameters on factors such as the polychaete population or actinospore release rate. The spatial and temporal distribution of actinospores in the river section is determined by their release from infected polychaetes at the hot spot, their decay and the dilution due to the river flow.

The spread of actinospores in the river is modelled by the following advection-reaction equation

$$\frac{\partial A}{\partial t} = \kappa P(x) - \delta(T)A - v_c \frac{\partial A}{\partial x}. \tag{5}$$

We assume that infected polychaetes P_0 only occur in river section II. We define the disease risk by the number of infected polychaetes P_0 in the river section. Referring to Ray et al. (2015), we define three different disease risk scenarios in each year:

high: $P_0 = 20,000$
medium: $P_0 = 15,200$
low: $P_0 = 7200$.

Note that $P(x) = P_0$ in zone II and $P(x) = 0$ elsewhere. At the boundaries of region II, we define $P(x = H_0) = P(x = H_L) = P_0$. We assume that the per-capita release rate κ of actinospores by polychaetes is constant during the salmon run. Deducted from Ray et al. (2015), we choose $\kappa = 9.750\,\mathrm{d}^{-1}$.

The relative decay rate δ of actinospores is described as a function of the water temperature T (Eq. (2)). Because the number of actinospores is very high, we assume that their reduction due to successful infection is negligible.

Since the current speed $v_c > 0$, we only have advective flux in the downstream direction and we choose an open boundary at the downstream end of the river section $\left(\left.\frac{\partial A}{\partial x}\right|_{x=L} = 0\right)$. We assume a dispersal barrier at the upstream boundary at IGD so that no spores can enter or leave the river. Therefore we choose a zero-flux boundary condition at $x = 0$ ($v_c A = 0$). The spatial steady-state solution for each zone can be found analytically (see Appendix A).

2.4. Salmon infection model

We assume that a pulse of susceptible salmon (S) migrates upstream with the relative migration velocity v_u. Salmon become infected to class I following uptake of actinospores and successful transmission with rate $\beta(T)$. After spawning, infected and susceptible salmon both die a natural death. However, infected adult carcasses produce myxospores that cause infection of juvenile salmon in the following spring. By predicting the infection prevalence in the adult salmon host, the infection risk of juvenile salmon in the following spring can be estimated. The Salmon infection model reads

$$\frac{\partial S}{\partial t} = -\beta(T)A(x)S - v_u(T, v_c)\frac{\partial S}{\partial x}, \tag{6}$$

$$\frac{\partial I}{\partial t} = +\beta(T)A(x)S - v_u(T, v_c)\frac{\partial I}{\partial x}. \tag{7}$$

The total number of salmon N is assumed to be constant during the migration period ($N = S + I$). We initialize the model with $S(t = 0) = N$ at the downstream boundary $x = L$ and end the simulation when all salmon reach the open boundary at $x = 0$. For the initial spatial distribution of actinospores $A(x)$, we take the equilibrium from Eq. (5).

Table 2
Analysed climate change and dam removal scenarios and the resulting influence on the infection prevalence. Temperature values are calculated from Perry et al. (2011) and discharge values from Greimann et al. (2011). The data in the last three columns indicate the relative increase of infection prevalence compared to the mean prevalence calculated for the years 2005–2013.

Climate change	Dams	T [°C]	Q [$m^3 s^{-1}$]	Relative increase of POI in %		
Scenario (GCM)			below IGD	P_0 = 7, 200	P_0 = 15, 200	P_0 = 20, 000
2005–2013 (median)	in	14.9	37.49	–	–	–
2012 (high prevalence in data and model)	in	17.1	28.77	51.33	19.38	10.95
warm/dry (MIUB)	in	17.5	36.81	49.10	18.94	10.80
	out	17.3	26.62	53.95	19.82	11.10
med/med (GFDL)	in	17.0	39.64	44.48	17.95	10.41
	out	16.8	33.98	45.09	18.09	10.47
cool/wet (MRI)	in	16.9	39.64	43.36	17.68	10.30
	out	16.6	33.98	42.08	17.37	10.18

3. Validation and analysis methods

3.1. Validation of the actinospore distribution model

To validate the actinospore distribution model, we compared its outcomes to more complex simulation model results from Bartholomew et al. (2016). With a detailed three dimensional hydrodynamic model of the Klamath River, that is presented and validated by Javaheri et al. (2018), they calculated concentration reduction of total spores (actinospores and myxospores) caused by an additional dam release ΔQ by using Lagrangian particle tracking. Since the ratio between actinospore and myxospore particles in their model is constant, we can use outcome of this complex hydrodynamic model to validate our actinospore distribution model.

Assuming a base flow of $Q = 30\,m^3 s^{-1}$ and $Q = 42\,m^3 s^{-1}$, we simulated the actinospore distribution model with an additional dam release ΔQ of 55, 110 and $170\,m^3 s^{-1}$ over 24 h with constant temperature. We then computed the actinospore reduction by comparing the total number of actinospores in the river section with additional dam release against the number with base flow and compared the outcome with the simulations of Bartholomew et al. (2016) by determining the R-squared value.

3.2. Validation of the salmon infection model

We validated our model against several studies (e.g. Bartholomew and Foott, 2010; Fogerty et al., 2012; Foott et al., 2010; 2016) where the prevalence of infection in returning Chinook salmon in the Klamath River was investigated in different calendar years (2005, 2006, 2009, 2011 and 2012). As input parameters, we took the mean temperature and discharge values in Klamath River in October in the year investigated (data obtained from the USGS National Water Information System https://waterdata.usgs.gov/). Since the total number of infected polychaetes in each year is unknown, we ran the simulations for the three defined disease risk cases (low/medium/high polychaete numbers).

3.3. Dam release scenarios

The results of the model of Bartholomew et al. (2016) show that an additional dam release can reduce the total spore concentration in the river by up to 50%. To evaluate the applicability of additional dam release just before the salmon run to reduce the infection prevalence, we tested our model system for different dam release scenarios. Similar to the validation of the actinospore distribution model, we simulated the model with an additional dam release ΔQ over 24 h assuming a base flow of $Q = 30\,m^3 s^{-1}$. With the resulting actinospore distribution $A(x)$, we simulated the salmon infection model with base flow. For both models (actinospore distribution and salmon infection model) the temperature was constant. We calculated the prevalence reduction due to additional flow by comparing the prevalence in the base flow scenario with the prevalence in the dam release scenario.

3.4. Climate change & dam removal scenarios

To estimate the impact of climate change and dam removal on the disease dynamics, we simulated the model for future environmental change scenarios and compared the resulting infection prevalence to current conditions. Future temperature changes in the Klamath River have been calculated for different climate change scenarios combined with dam removal options simulated by Perry et al. (2011). Future discharge values for these scenarios in the study area have been calculated from Greimann et al. (2011). From these studies, we selected three climate change scenarios: the MIUB (Meteorological Institute of the University of Bonn) - warm/dry scenario, the MRI (Meteorologic Research Institute) - cool/wet scenario and the GFDL (Geophysical Fluid Dynamics Laboratory) scenario for medium precipitation and temperatures. For a reference run, we took the median of the temperature and discharge values of the years 2005 – 2013. Furthermore, we compared the result of the reference run to the data of the year 2012 since our model produces the maximum prevalence for given temperature and discharge during the years 2005 – 2013 in 2012. Each of the climate change and dam removal scenarios was run for each of the three disease risk scenarios. An overview of the analysed scenarios can be found in Table 2.

3.5. Dose-response model

To approximate the infection risk of returning salmon population, we developed a dose-response model for *Ceratomyxosis*. Typically, the parameters of these models are found empirically by dosing experiments in which pathogen doses are varied and the host's response is monitored (Haas, 1996). With the exponential dose-response model, the prevalence of infection POI in its general form is given by

$$POI = 1 - \exp(-kD), \tag{8}$$

where k is the probability to successfully initiate a response and D the dose of the substance or pathogen. By using the methods of characteristics, we will show that our model system can be reduced to a single equation, which is equivalent to the exponential dose-response model.

4. Results

4.1. Actinospore distribution model

As mentioned above, a steady state solution for the spatial distribution of actinospores can be found analytically (see Appendix A).

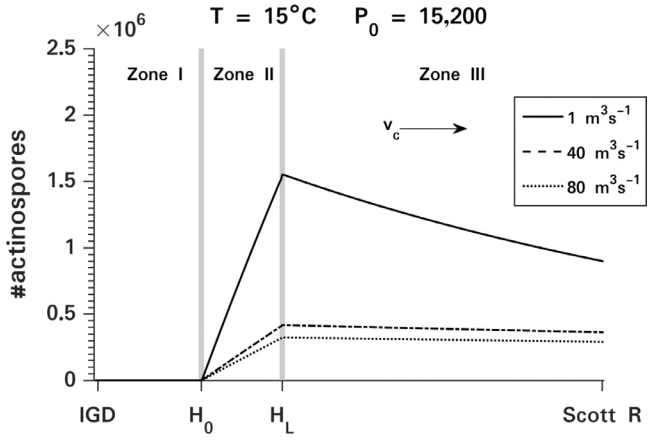

Fig. 6. Spatial steady state distribution of actinospores released in zone II at $T = 15\,°C$ and a polychaete number $P_0 = 15,200$. For higher discharges Q, the number of actinospore decreases (shown in different lines). The borders of the zones are indicated by grey lines. The steady state solution for each zone can be found analytically (see Appendix A).

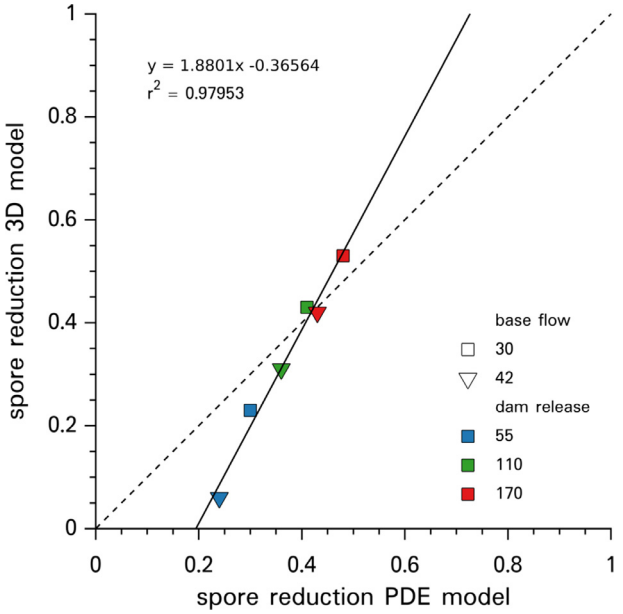

Fig. 8. Validation of the actinospore distribution model: The horizontal axis shows the reduction of actinospore concentration for various dam release scenarios simulated with the actinospore distribution model (Section 2.3); the vertical axis shows the concentration reduction of spores for the same scenarios investigated by Bartholomew et al. (2016). The dashed line is the line that bisects the x- and y-axis; the solid line depicts the slope of the linear fit.

Fig. 6 shows the distribution for a fixed temperature of $T = 15\,°C$ and polychaete number $P_0 = 15,200$ (medium disease risk). The number of actinospores is zero in zone I, increases in their release zone II (the polychaete habitat) and decreases exponentially up to the confluence with Scott River (zone III). For a higher discharge Q the number of actinospores decreases and the exponential decrease in zone III is less marked. For $P_0 = 7,200$ and $P_0 = 20,000$ (low and high disease risk, respectively), the stationary spatial distributions are qualitatively similar. The total number of actinospores in the river section decreases with increasing temperature, but is more sensitive to changes in the discharge (Fig. 7). The higher the number of polychaetes, the higher the number of actinospores.

Total spore reduction due to dam release in the 3D model by Bartholomew et al. (2016) ranges from 6% to 53%, depending on the base flow and dam release. In the PDE model introduced by the current study, the actinospore reduction ranges from 24% to 48% (Fig. 8). In total, the simulations of our PDE model show a very good correlation with the detailed hydrodynamic model ($R^2 = 0.9795$).

4.2. Salmon infection model

The salmon infection model has been used to calculate the infection prevalence in returning adult salmon. The prevalence of infection (POI) is herein defined as the proportion of infected fish (I/N) arriving at the spawning area at IGD at $x = 0$. In a high disease risk year ($P_0 = 20,000$), the prevalence is close to one for temperatures above $T = 15\,°C$ and decreases with decreasing temperatures (Fig. 9). For all simulated polychaete numbers, the maximum prevalence occurs at $T = 18\,°C$, corresponding to the maximum of the transmission rate β (Eq. (4)). In accordance with the number of actinospores in the river section (Fig. 7), prevalence decreases with increasing river discharge for all three cases of disease risk. However this trend is less pronounced than that of temperature. The lower the number of polychaetes, the lower the maximum of POI.

For each simulated year, the measured prevalence data is within the range predicted by the infection model (Fig. 10). For three data points, the model shows an excellent correlation with the data points for a medium number of polychaetes.

4.3. Dam release scenarios

The resulting prevalence reduction due to additional water flow is shown in Fig. 11. The results indicate that the higher the additional

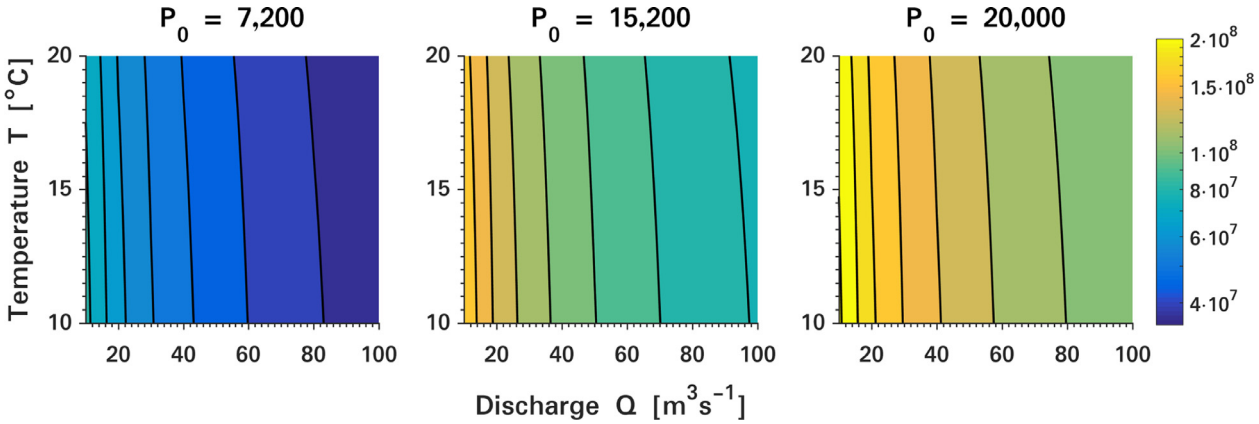

Fig. 7. Total number of actinospores in the river section as a function of temperature and discharge. The left panel shows the number of actinospore for a low polychaete numbers, the middle for a medium and the right for a high polychaete numbers.

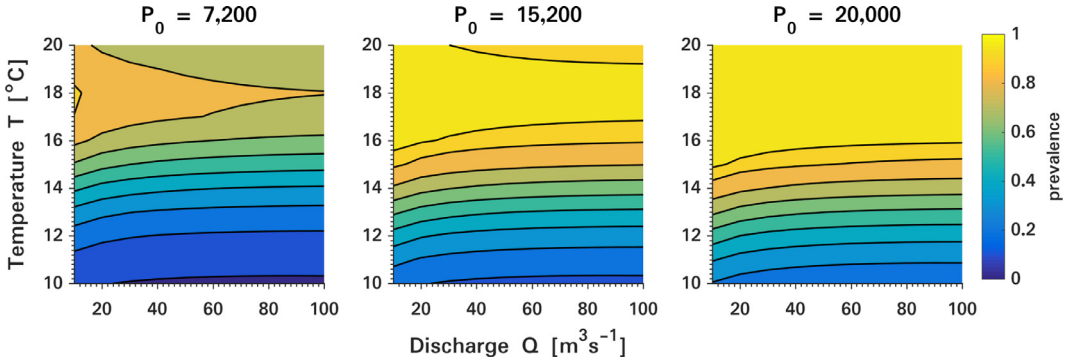

Fig. 9. Prevalence of infection obtained by the infection model (Section 2.4) as a function of temperature and discharge for low (left panel), medium (middle) and high (right) polychaete numbers.

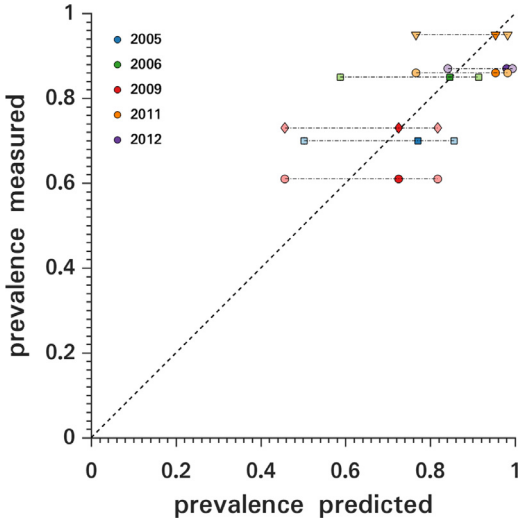

Fig. 10. Validation of the infection model: *x*-coordinate shows the predicted prevalence obtained by the PDE model of this study. The y-coordinate shows the prevalence of infection in returning salmon measured by several studies. Different colours indicate different years of measurements. The results of the PDE model for each year with different polychaeta densities are connected by a dashed line. The darker point of each connection corresponds to a medium polychaeta density. The symbols refer to different datasets: (▽) Fogerty et al. (2012); (◦) Foott et al. (2016); (⋄) Foott et al. (2010); (□) Bartholomew and Foott (2010). Symbols from left to right on a dashed line: low (7200), medium (15,200), high (20,000) polychaeta density.

dam release, the higher the resulting prevalence reduction. The dam release is more effective if the number of polychaetes in the river section is low. A dam release of $\Delta Q = 125\,\mathrm{m}^3 s^{-1}$ at temperatures below $T = 14\,°\mathrm{C}$ can result in a prevalence reduction up to 35%. For high polychaete numbers and temperatures around $T = 18\,°\mathrm{C}$ even a high additional discharge has nearly no effect on infection prevalence.

4.4. Climate change & dam removal scenarios

Compared to the climate conditions of the years 2005 – 2013, climate change is likely to increase the prevalence of infection significantly (Table 2). For high polychaete numbers, infection prevalence is 90% in the reference run (Fig. 9). Yet, climate change and dam removal still increase prevalence by 10%. The calculated prevalences of all scenarios are comparable to those in the high prevalence year of 2012. Since the infection prevalence for future climate conditions is high anyhow, dam removal seems to have little quantitative effect on the prevalence. While dam removal increases prevalences in the warm/dry and med/med scenarios, it decreases prevalences in the cool/wet scenarios. For low disease risk, the simulated scenarios predict an increase of prevalence by 42–54%.

4.5. Dose-response model

From the solution of the salmon infection model (Eq. (6)), we can derive the exponential dose-response model (see Appendix B). With the mean spatial actinospore dose $\overline{A}$ over the river section we can calculate the prevalence of infection as

$$POI = 1 - \exp(-\beta(T)\tau(T, v_c)\overline{A}). \tag{9}$$

With the existing empirical description of the transmission rate β

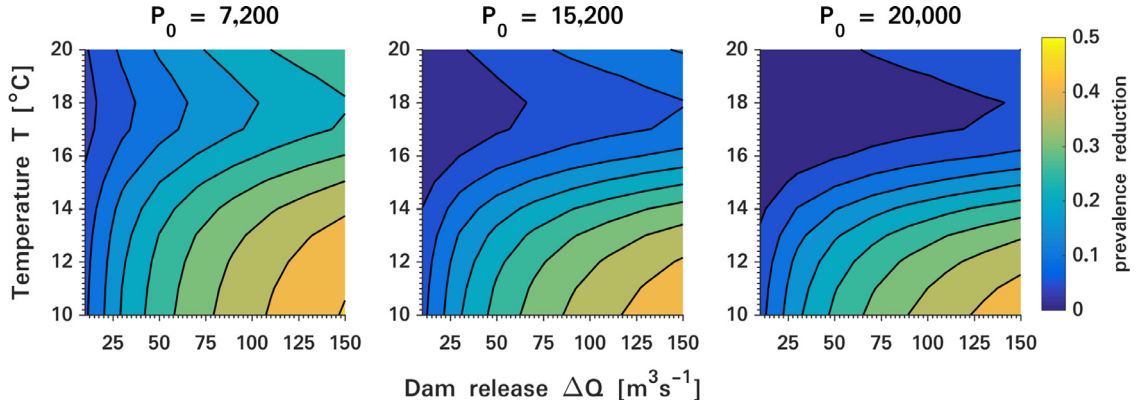

Fig. 11. Prevalence reduction in returning salmon as a function of temperature and additional dam release ΔQ. In the scenarios, we assume a base flow of $Q = 30\,\mathrm{m}^3 s^{-1}$ for the actinospore and salmon infection model and an additional dam release ΔQ over 24 h for the actinospore model. The panels show the results for low (left panel), medium (middle) and high (right) polychaete numbers.

(Eq. (4)), the travel time τ (Eq. (3)) and *in-situ* measurement of the mean actinospore concentration $\overline{A}$, the infection risk of the years returning salmon population can be approximated easily, without simulating the entire presented PDE model. Therefore, the dose-response model is suitable as a decision support tool in disease management. Moreover, it is also applicable for downstream migrating juvenile salmon by adapting the formulations and parameters of the transmission rate and the travel time to the physiology of juvenile salmon.

5. Discussion and conclusion

Declining populations of Chinook salmon caused by fish diseases are a serious ecological and economic problem in the Pacific Northwest. In order to aid disease control and mitigation, it is necessary to predict the impact of changing water temperatures and flow regimes, whether caused by climate change or dam removal. We developed a model including empirical formulations of transmission rate and migration speed to estimate the infection prevalence of *Ceratomyxosis* in returning salmon. The model results and the scenario analyses provide useful information on how changing river discharge and temperature affect or can be used to affect the infection risk.

The model results and scenario analyses show that changing environmental conditions have different effects on the disease components: The actinospore concentration is more sensitive to changing discharge than to changing temperatures. In contrast, the prevalence of infection is more sensitive to changes in temperatures. As the actinospore distribution feeds into the infection model, this is likely to be caused by the temperature dependence of the transmission rate (Fig. 2). Compared to our calculated prevalence of infection, the mortality rate of juvenile salmon modelled by Fujiwara (2014) shows a higher sensitivity to changes in discharge. In contrast to our empirically based formulation of the temperature dependence of the infection rate, based on the studies of Ray and Bartholomew (2013), he assumes an exponential increase in infection rate with increasing temperature. Furthermore, we included the temperature dependence in the decay rate of the actinospores and the temperature-dependent travel time of salmon that both have not been considered by Fujiwara (2014).

5.1. Climate change

We investigated the influence of future environmental change scenarios and showed that the prevalence of infection for future climate change scenarios in comparison to current conditions is likely to increase. Depending on the disease risk in terms of infected polychaete, the increase ranges from 10 – 54%. These predictions are consistent across the climate change scenarios investigated. Predicted infection prevalences are comparable to those of recent high-disease years. Similar, Ray et al. (2015) predicted a high mortality in juvenile salmon for nearly all future climate scenarios. Since host-parasite dynamics are complex, the total effect of environmental change on disease dynamics is hard to predict. On the one hand, increasing water temperature could increase or decrease infection prevalence, depending on the current temperature and the number of infected polychaetes (Fig. 9). Higher temperatures can also lead to shifts in the invertebrate host distribution (Alexander et al., 2014) or in timing and duration of spore production and host-parasite interaction (Ray et al., 2015). Moreover, temperatures in Klamath River are already at the salmon's upper thermal limit (Ray et al., 2015), which makes the future of the salmon population in the river unclear. On the other hand, different water flows affect the spore concentration (Fig. 7) and travel time of salmon (Fig. 4). In addition, varying effects related to changing temperatures will interact with changes brought about different water flows.

5.2. Dam removal

Most of the world's large river systems are fragmented by dams (Nilsson et al., 2005). On the one hand, this fragmentation is likely to increase due to a global boom in hydropower dam with at least 3700 major dams currently planned or in construction (Zarfl et al., 2015). On the other hand, there are attempts to restore river ecosystems by removing dams. Consequently, the ecological effects of undamming rivers is of great interest (e.g. Bednarek, 2001; Poff and Hart, 2002; Stanley and Doyle, 2003).

Due to its relatively small predicted effect on temperature in comparison to the impact of climate change, our model suggests that dam removal is more likely to have little influence on the predicted level of infection (Table 2). Based on our scenario analysis with our model as parameterized, we conclude that dam removal has little effect on the amelioration of climate change on infection prevalence. Since the model is more sensitive to changes in temperature than to changes in discharge, the significant effect of dam removal on discharge, in combination with increasing temperature due to climate change, does not translate into having an impact on our simulated infection prevalence. However, if other factors were included (e.g. the influence of environmental parameters on the polychaete's life cycle or temporal and spatial variation of the host-parasite interactions) then it could be possible that the conclusions would be changed.

Our results related to dam removal have to be interpreted with caution. In particular, dam removal not only alters water temperatures and flow, but will also change the spatial overlap between the host and parasites. Migration of salmon to the upper Klamath basin after dam removal could provide new hosts for existing parasite genotypes that are currently isolated upstream of the dams. Similarly, migrating salmon could transport new pathogenic genotypes of *C. shasta* to currently isolated salmon populations in the upper basin (Hurst et al., 2012). In addition, the influence of environmental parameters on the polychaete's life cycle is not yet understood (Stocking and Bartholomew, 2007). As we discussed before, changing environmental conditions like water temperature could lead to a range shift of the invertebrate host distribution. The polychaete density P_0 or the release rate κ, for example, could be functions of the water temperature.

5.3. Flow manipulation

It has been shown elsewhere that flow manipulation can be used for reducing the polychaete density (Alexander et al., 2014) or the spore concentration (Bartholomew et al., 2016). Other management options, as for instance removing adult carcasses to reduce the myxospore input (Foott et al., 2016), have been shown to have little effect on the infection risk. Our model results show that dam release before the salmon run can reduce the actinospore concentration as well as the infection prevalence in returning salmon and can therefore be a useful tool for managing Ceratomyxosis.

5.4. Perspective

We showed that our model, although based on a number of mechanistic subprocesses, can be simplified to an exponential dose-response function that can be integrated in decision support systems. Despite the simplicity of this function, it encapsulates all significant mechanisms of the disease dynamics in adult fish considered here. This simplicity is one of the greatest advantages of our model. In principle, one needs only three measurements to predict the infection risk of the returning salmon population in a given year: water temperature, discharge and actinospore concentration. The analysis we presented here for Ceratomyxosis in the Klamath River is easily applicable to other fish diseases at different locations. For instance, the myxozoan parasite *Myxobolis cerebralis*, the causing agent of whirling disease, has a life cycle that is similar to *C. shasta*. Discharge, temperature and spore concentration are easy to measure and can be used to estimate the infection risk with the dose-response model and evaluate the effectiveness of disease management options.

Acknowledgement

We thank Michael Bengfort, Gunnar Niebaum and Karsten Lettmann for their inputs and useful comments on this paper. MAL gratefully acknowledges an Natural Sciences and Engineering Research Council of Canada Discovery grant and a Canada Research Chair.

Appendix A. Analytic solution for actinospore distribution model

In the actinospore distribution model (Eq. (5)), we defined the distribution of infected polychaete as $P(x) = P_0$ in zone II and $P(x) = 0$ elsewhere. Let $0 \le x \le L$ be the reach of the total modelled area and $H_0 \le x \le H_L$ the reach of zone II. We set $A(x = 0) = 0$ on the upstream boundary at IGD.

For zone I ($x < H_0$; $P(x) = 0$) and zone III ($x > H_L$; $P(x) = 0$), we have a homogeneous ODE where the steady state solution for the actinospore distribution is $A^*(x) = A_0^* \exp\left(-\frac{\delta(T)}{v_c}x\right)$ where A_0^* is a constant defined by the initial value at the beginning of each zone. With the upstream boundary condition we obtain for zone I $A_I^*(x) = 0$.

For zone II ($H_0 \le x \le H_L$; $P(x) = P_0$), we derive the steady state solution by using the method of variation of parameters:

$$A_{II}^*(x) = \frac{\kappa P_0}{\delta(T)} + c' \exp\left(-\frac{\delta(T)}{v_c}x\right). \tag{A.1}$$

To match the actinospore numbers from zone I, we impose the boundary conditions $A^*(x = H_0) = 0$ and derive for the constant c'

$$c' = -\frac{\kappa P_0}{\delta(T)} \exp\left(\frac{\delta(T)}{v_c}H_0\right).$$

Consequently, our steady state solution for zone II is

$$A_{II}^*(x) = \frac{\kappa P_0}{\delta(T)}\left[1 - \exp\left(\frac{\delta(T)}{v_c}(H_0 - x)\right)\right].$$

Matching this equation with the boundary condition of zone III we obtain

$$A^*(H_L) = \frac{\kappa P_0}{\delta(T)}\left[1 - \exp\left(\frac{\delta(T)}{v_c}(H_0 - H_L)\right)\right] = A_0^* \exp\left(-\frac{\delta(T)}{v_c}x\right).$$

It follows

$$A_0^* = \frac{\kappa P_0}{\delta(T)}\left[\exp\left(\frac{\delta(T)}{v_c}H_L\right) - \exp\left(\frac{\delta(T)}{v_c}H_0\right)\right]$$

and we finally derive for zone III

$$A_{III}^*(x) = \frac{\kappa P_0}{\delta(T)}\left[\exp\left(\frac{\delta(T)}{v_c}(H_L - x) - \exp\left(\frac{\delta(T)}{v_c}(H_0 - x)\right)\right)\right]. \tag{A.2}$$

In summary we have the following solution for the spatial distribution of the actinospores:

$$A^*(x) = \begin{cases} 0 & \text{if} \quad x < H_0\,, \\ \kappa\frac{P_0}{\delta(T)}\left[1 - \exp\left(\frac{\delta(T)}{v_c}(H_0 - x)\right)\right] & \text{if} \quad H_0 \le x \le H_L\,, \\ \kappa\frac{P_0}{\delta(T)}\left[\exp\left(\frac{\delta(T)}{v_c}(H_L - x)\right) - \exp\left(\frac{\delta(T)}{v_c}(H_0 - x)\right)\right] & \text{if} \quad x > H_L\,. \end{cases}$$

Appendix B. Derivation of the dose-response model from the salmon infection model

Here, we want to determine the proportion of infected fish and thus the prevalence of infection $POI = I/N$, at the end of the simulation. We assume the temperature T and the water velocity v_c to be constant so that $\beta(T) = \beta$ and $v_u(T, v_c) = v_u$. In a first step we solve Eq. (6) by using the Method of Characteristics. Considering the general transportation problem

$$P(x, t)\frac{\partial S}{\partial t} + Q(x, t)\frac{\partial S}{\partial x} + R(x, t)S = 0 \tag{B.1}$$

we derive $P(x, t) = 1$, $Q(x, t) = v_u$ and $R = \beta A(x)$ as characteristic equations for Eq. (6). We introduce the variable T' so that the PDE reduces to an ODE on $x(T')$ and $t(T')$ if $T' > 0$. We choose

$$\frac{\partial t}{\partial T'} = P(x, t) = 1$$

and

$$\frac{\partial x}{\partial T'} = Q(x, t) = v_u$$

so that we can write

$$\frac{dS}{dT'} = \frac{\partial S}{\partial x}\frac{dx}{dT'} = \frac{\partial S}{\partial t}\frac{dt}{dT'} = Q(x,t)\frac{\partial S}{\partial x} + P(x,t)\frac{\partial S}{\partial t} = -R(x,T')S\,.$$

This ODE can be solved as follows:

$$S(T') = S(0)\exp\left(\int_0^{T'} -\beta A(x(t))dt\right). \tag{B.2}$$

At the end of the simulation T'_{end} we have

$$\begin{aligned} S(T'_{end}) &= S(0)\exp\left(\frac{-\beta}{v_u}\int_0^L A(x)dx\right) \\ &= S(0)\exp\left(\frac{-\beta}{L}\tau\int_0^L A(x)dx\right) \\ &= S(0)\exp(-\beta\tau\overline{A})\,. \end{aligned}$$

Since $N(T'_{end}) = S(T'_{end}) + I(T'_{end})$ and $S(0) = N$ we can write

$$\begin{aligned} I &= N - S \\ &= N - N\exp(-\beta\tau\overline{A})\,, \end{aligned}$$

and we get finally the proportion of infected fish in the total population by

$$\frac{I}{N} = 1 - \exp(-\beta\tau\overline{A})\,. \tag{B.3}$$

References

Alexander, J.D., Hallett, S.L., Stocking, R.W., Xue, L., Bartholomew, J.L., 2014. Host and parasite populations after a ten year flood: manayunkia speciosa and ceratonova (syn Ceratomyxa) shasta in the Klamath River. Northwest Sci. 88 (3), 219–233.

Bartholomew, J.L., Atkinson, S.D., Hallett, S.L., Zielinski, C.M., Foott, J.S., 2007. Distribution and abundance of the salmonid parasite Parvicapsula minibicornis (Myxozoa) in the Klamath River basin (Oregon-California, U.S.A.). Dis. Aquatic Organ. 78 (2), 137–146.

Bartholomew, J.L., Foott, J.S., 2010. Compilation of Information Relating to Myxozoan Disease Effects to Inform the Klamath Basin Restoration Agreement. Technical Report. Department of Microbiology, Oregon State University.

Bartholomew, J.L., Hallett, S.L., Holt, R.A., Alexander, J.D., Atkinson, S.D., Buckles, G.R., Craig, R., Javaheri, A., Babar-Sebens, M., 2016. Klamath River Fish Health: Disease Monitoring and Study. Technical Report. Oregon State University.

Bednarek, A.T., 2001. Undamming rivers: a review of the ecological impacts of dam removal. Environ. Manag. 27 (6), 803–814.

Bjork, S.J., 2010. Factors Affecting the Ceratomyxa shasta Infectious Cycle and Transmission between Polychaete and Salmonid Hosts. Oregon State University Dissertation.

Bjork, S.J., Bartholomew, J.L., 2009. The effects of water velocity on the Ceratomyxa shasta infectious cycle. J. Fish Dis. 32 (2), 131–142.

Fogerty, R., Foott, J.S., Stone, R., Bolick, A., True, K., 2012. Ceratomyxa Shasta Myxospore Survey of Fall-run Chinook Salmon Carcasses in the Klamath and Shasta Rivers, and Bogus Creek, 2011. Technical Report. U.S. Fish and Wildlife Service, California Nevada Fish Health Center, Anderson, CA.

Foott, J.S., Fogerty, R., Stone, R., 2010. Ceratomyxa Shasta Myxospore Survey of Fall-run Chinook Salmon Carcasses in Bogus Creek, Shasta River and Klamath River: Component of Joint OSU-Yurok Fisheries-CDFG Pilot Project Testing the Effect of Carcass Removal on C. Shasta Myxospore Levels in Bogus Creek, 2009–2010. Technical Report. U.S. Fish and Wildlife Service, California Nevada Fish Health Center, Anderson, CA.

Foott, J.S., Stone, R., Fogerty, R., True, K., Bolick, A., Bartholomew, J.L., Hallett, S.L., Buckles, G.R., Alexander, J.D., 2016. Production of ceratonova shasta myxospores from salmon carcasses: carcass removal is not a viable management option. J. Aquatic Anim. Health 28 (2), 75–84.

Foott, J.S., Stone, R., Wiseman, E., True, K., Nichols, K., 2007. Longevity of Ceratomyxa shasta and parvicapsula minibicornis actinospore infectivity in the Klamath River. J. Aquatic Anim. Health 19 (2), 77–83.

Fujiwara, M., 2014. Dynamics of infection of juvenile chinook salmon with Ceratomyxa shasta. Fisheries Aquac. J. 05 (01).

Fujiwara, M., Mohr, M.S., Greenberg, A., Foott, J.S., Bartholomew, J.L., 2011. Effects of ceratomyxosis on population dynamics of Klamath fall-run chinook salmon. Trans. Am. Fisheries Soc. 140 (5), 1380–1391.

Govers, G., 1992. Relationship between discharge, velocity and flow area for rills eroding loose, non-layered materials. Earth Surf. Proces. Landf. 17 (5), 515–528.

Greimann, B.P., Varyu, D., Godaire, J., Russell, K., Lai, Y.G., Talbot, R., King, D., 2011. Hydrology, Hydraulics and Sediment Transport Studies for the Secretary's Determination on Klamath River Dam Removal and Basin Restoration. Technical Report No. SRH-2011–02. Bureau of Reclamation, Mid-Pacific Region, Technical Service Center, Denver, Colorado.

Haas, C.N., 1996. How to average microbial densities to characterize risk. Water Res. 30 (4), 1036–1038.

Haas, C.N., Rose, J.B., Gerba, C.P., 1999. Quantitative Microbial Risk Assessment. John Wiley & Sons, New York, NY.

Hallett, S.L., Bartholomew, J.L., 2011. Myxobolus cerebralis and Ceratomyxa shasta. In: Woo, P., Buckmann, K. (Eds.), Fish Parasites: Pathobiology and Protection. CAB International, Wallingford.

Hallett, S.L., Ray, R.A., Hurst, C.N., Holt, R.A., Buckles, G.R., Atkinson, S.D., Bartholomew, J.L., 2012. Density of the waterborne parasite Ceratomyxa shasta and its biological effects on salmon. Appl. Environ. Microbiol. 78 (10), 3724–3731.

Huang, Y., Haas, C.N., 2009. Time-dose-response models for microbial risk assessment. Risk Anal. 29 (5), 648–661.

Hurst, C.N., Holt, R.A., Bartholomew, J.L., 2012. Dam removal and implications for fish health: Ceratomyxa shasta in the Williamson River, Oregon, USA. North Am. J. Fisheries Manag. 32 (1), 14–23.

Javaheri, A., Babbar-sebens, M., Alexander, J., Bartholomew, J., Hallett, S., 2018. Global sensitivity analysis of water age and temperature for informing salmonid disease management. J. Hydrol. 561, 89–97.

Jones, S.R.M., Bartholomew, J.L., Zhang, J.Y., 2015. Mitigating myxozoan disease impacts on wild fish populations. In: Okamura, B., Gruhl, A., J., B. (Eds.), Myxozoan Evolution, Ecology and Development. Springer International Publishing, Cham, pp. 397–413.

Nilsson, C., Reidy, C.A., Dynesius, M., Revenga, C., 2005. Fragmentation and flow regulation of the world's large river systems. Science 308, 405–408.

Okamura, B., Gruhl, A., Bartholomew, J.L., 2015. An introduction to myxozoan evolution, ecology and development. In: Okamura, B., Gruhl, A., J.L., B. (Eds.), Myxozoan Evolution, Ecology and Development. Springer International Publishing, Cham, pp. 1–20.

Perry, R.W., Risley, J.C., Brewer, S.J., Jones, E.C., Rondorf, D.W., 2011. Simulating Daily Water Temperatures Of the Klamath River Under dam Removal and Climate Change Scenarios. Open-File Report 2011–1243. US Geological Survey.

Poff, N.L., Hart, D.D., 2002. How dams vary and why it matters for the emerging science of dam removal. BioScience 52 (8), 659–668.

Ray, R.A., 2013. Modeling Abiotic Influences on Disease Dynamics for the Complex Life Cycle of the Myxozoan Parasite Ceratomyxa shasta. Oregon State University Dissertation.

Ray, R.A., Alexander, J.D., De Leenheer, P., Bartholomew, J.L., 2015. Modeling the effects of climate change on disease severity: a case study of ceratonova (syn Ceratomyxa) shasta in the Klamath River. In: Okamura, B., Gruhl, A., J.L., B. (Eds.), Myxozoan Evolution, Ecology and Development. Springer International Publishing, Cham, pp. 363–378.

Ray, R.A., Bartholomew, J.L., 2013. Estimation of transmission dynamics of the Ceratomyxa shasta actinospore to the salmonid host. Parasitology 140 (07), 907–916.

Salinger, D.H., Anderson, J.J., 2006. Effects of water temperature and flow on adult salmon migration swim speed and delay. Trans. Am. Fisheries Soc. 135 (1), 188–199.

Standen, E.M., Hinch, S.G., Rand, P.S., 2004. Influence of river speed on path selection by migrating adult sockeye salmon (Oncorhynchus nerka). Can. J. Fisheries Aquatic Sci. 61, 905–912.

Stanley, E.H., Doyle, M.W., 2003. Trading off: the ecological effects of dam removal. Front. Ecol. Environ. 1 (1), 15–22.

Stocking, R.W., Bartholomew, J.L., 2007. Distribution and habitat characteristics of manayunkia speciosa and Infection prevalence with the Parasite Ceratomyxa shasta in the Klamath River, Oregon-California. J. Parasitol. 93 (1), 78–88.

Stocking, R.W., Holt, R.A., Foott, J.S., Bartholomew, J.L., 2006. Spatial and temporal occurrence of the salmonid parasite Ceratomyxa shasta in the Oregon-California Klamath River Basin. J. Aquatic Anim. Health 18 (3), 194–202.

Teunis, P.F.M., Nagelkerke, N.J.D., Haas, C.N., 1999. Dose response models for infectious gastroenteritis. Risk Anal. 19 (6), 1251–1260.
True, K., Bolick, A., Foott, J.S., 2011. Myxosporean parasite (Ceratomyxa shasta and Parvicapsula minibicornis) annual prevalence of infection in Klamath River basin juvenile Chinook salmon, Apr-Aug 2010. Technical Report. U.S. Fish and Wildlife Service, California Nevada Fish Health Center, Anderson, CA.
Udey, L.R., Fryer, J.L., Pilcher, K.S., 1975. Relation of water temperature to ceratomyxosis in rainbow trout (salmo gairdneri) and coho salmon (oncorhynchus kisutch). J. Fisheries Res. Board Can. 32 (9), 1545–1551.
Watanabe, T., Bartrand, T.A., Omura, T., Haas, C.N., 2011. Dose-response assessment for influenza a virus based on data sets of infection with its live attenuated reassortants. Risk Anal. 32 (3), 555–565.
Watanabe, T., Bartrand, T.A., Weir, M.H., Omura, T., Haas, C.N., 2010. Development of a dose-response model for SARS coronavirus. Risk Anal. 30 (7), 1129–1138.
Zarfl, C., Lumsdon, A.E., Berlekamp, J., Tydecks, L., Tockner, K., 2015. A global boom in hydropower dam construction. Aquatic Sci. 77 (1), 161–170.